

Competing interactions and anisotropic magnetoresistance in layered CeTe₂

M. H. Jung, K. Umeo, T. Fujita, and T. Takabatake

Department of Quantum Matter, ADSM, Hiroshima University, Higashi-Hiroshima 739-8526, Japan

(Received 23 May 2000)

On a single crystal of CeTe₂ with a layered tetragonal structure, we have studied the effect of magnetic field on magnetic susceptibility M/B , specific heat C , and electrical resistivity ρ . It is confirmed that this compound orders antiferromagnetically at $T_N=4.4$ K, while $\rho(T)$ shows no anomaly at T_N but a sharp peak at $T_\rho=6.1$ K. Below T_ρ , M/B rises suddenly for $B\parallel c$, the easy magnetization axis, suggesting the onset of a short-range ferromagnetic order. At 2 K, $M(B\parallel c)$ shows a metamagnetic transition at a small field of 0.06 T from the antiferromagnetic ground state to a field-induced ferromagnetic state. The peak in $C(T)$ shifts from 4.3 K in zero field to 4.0 K in $B_{\parallel c}=0.1$ T, and furthermore a shoulder appears at 4.3 K. With increasing magnetic field, the shoulder changes to a broadened maximum, which shifts towards higher temperatures. These observations indicate that the ferromagnetic interaction competes with the antiferromagnetic one even in zero field. A large negative magnetoresistance, $MR=[\rho(B)-\rho(0)]/\rho(0)$, was observed in the vicinity of T_ρ . For $I\parallel c$, the MR amounts to -25% at 3 T for $B\parallel c$, which is twice that for $B\perp c$. The large MR for $I\parallel B\parallel c$ is a result of the increase of the c -axis conduction in the field-induced ferromagnetic alignment of Ce spins. However, the MR for $I\perp c$ is essentially the same for $B\parallel c$ and $B\perp c$, suggesting the confinement of carriers within the Te sheet sandwiched by the ferromagnetically coupled CeTe layers.

I. INTRODUCTION

Rare-earth based compounds with layered crystal structures such as RX_n (R =rare earth; X =S, Se, Te, $n=2,2.5,3$) (Refs. 1 and 2) and RSb_2 (R =La-Nd and Sm) (Refs. 3 and 4) exhibit highly anisotropic transport and magnetic properties. The compounds RTe_2 crystallize in the layered Cu₂Sb-type tetragonal structure.⁵ Among this series, CeTe₂ has been studied extensively.⁶⁻¹² This compound is constructed from semiconducting CeTe double layers separated by a semimetallic Te sheet stacking along the c axis, and thus exhibits high anisotropy in transport and magnetic properties.^{9,12-14} For example, the c -axis resistivity $\rho_{\parallel c}$ exhibits a semiconducting temperature dependence of the order of a few tens Ω cm, while the c -plane resistivity $\rho_{\perp c}$ shows a broad maximum at 100 K and then decreases on cooling, resulting in the resistivity ratio $\rho_{\parallel c}/\rho_{\perp c}\sim 150$ at 1.5 K. The large resistivity even in the c plane has been attributed to the presence of charge-density wave (CDW), with a pseudogap of 0.35 eV.⁹ Electron-tunneling measurements suggested that the CDW transition temperature is far above room temperature.

CeTe₂ undergoes an antiferromagnetic transition at $T_N=4.3$ K,^{6,9} where both magnetic susceptibility $\chi(T)$ and specific heat $C(T)$ exhibit a peak. However, $\rho(T)$ shows a sharp peak at $T_\rho=6.1$ K well above $T_N=4.3$ K, which was explained in terms of ferromagnetic-type magnetic polarons.^{9,12} In this picture, the carriers of $5p$ electrons in the Te sheet become localized well above the long-range magnetic order at T_N because their spins are coupled to the Ce spins via local ferromagnetic exchange interactions. The short-range ferromagnetic order was indicated by the marked increase of $C(T)$ below 10 K. Recent elastic and inelastic neutron-scattering studies revealed two successive transitions at temperatures T_ρ and T_N .^{10,11} From the sudden decrease in the a -axis lattice parameter below T_ρ , it was proposed that the

transition at T_ρ has magnetoelastic origin. Below T_ρ the magnetic moments of Ce ions are partially aligned ferromagnetically in a CeTe layer, and below T_N the ferromagnetic layers are stacked antiferromagnetically in the spin sequence up-down-down-up along the c axis. It is now conjectured that the short-range ferromagnetic order is responsible for the drop in $\rho(T)$ at $T\leq T_\rho$.

Our previous measurements of $\rho(T)$ for polycrystalline samples of CeTe₂ in various magnetic fields showed that the peak in $\rho(T)$ at $T_\rho=6.1$ K in zero field is strongly depressed with increasing field and the peak temperature shifts gradually towards higher temperatures for both the longitudinal and transverse configurations.^{6,9} This shift to higher temperatures is opposite to that of the peak in $\chi(T)$. It should be noted that the magnetoresistance, $MR=[\rho(B)-\rho(0)]/\rho(0)$, is the largest in the vicinity of 6.1 K. The negative MR for $B<0.2$ T accompanies a rapid rise of the initial magnetization curve $M(B)$. This fact suggested that the negative MR is closely associated with the ferromagnetic moments induced by the magnetic field. Furthermore, one can expect anisotropic $\rho(B)$ and $M(B)$ in response to the direction of magnetic field for $B\parallel c$ and $B\perp c$, because the layered magnetic structure in CeTe₂ is similar in some sense to magnetic multilayers showing giant magnetoresistance.¹⁵ In this paper, we report on magnetic-field variations of $\chi(T)$, $C(T)$, and $\rho(T)$ on a single crystal of CeTe₂.

II. EXPERIMENTAL DETAILS

Samples of CeTe₂ were prepared by the mineralization method, as described previously.⁹ Powder x-ray-diffraction patterns indicated that the samples are almost single phased with the tetragonal Cu₂Sb-type structure with the lattice parameters $a=4.47$ Å and $c=9.11$ Å. Electron-probe microanalysis of several parts of the samples showed that the compositions in the host phase are deficient in Te content,

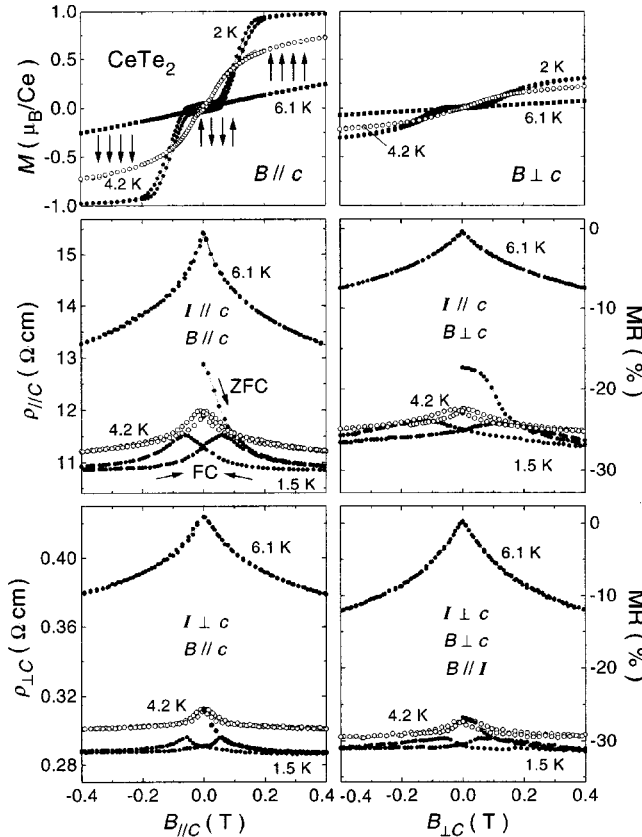


FIG. 1. (Top) isothermal magnetization of a single crystal of CeTe_2 for $B\parallel c$ and $B\perp c$ measured at temperatures 2, 4.2, and 6.1 K. The arrows indicate the direction of Ce spins in the two CeTe double layers. Middle and bottom panels show, respectively, field-dependent resistivity of CeTe_2 for $I\parallel c$ and $I\perp c$ at 1.5, 4.2, and 6.1 K upon increasing and decreasing magnetic field. Magnetoresistance, $\text{MR}=[\rho(B)-\rho(0)]/\rho(0)$ at 6.1 K is shown by the right-hand axis.

$\text{CeTe}_{1.85}$. By cleaving the samples, single crystals of the size $1.0\times 1.0\times 0.5\text{ mm}^3$ with (001) surfaces were obtained.

Because of the platelike shapes of the single crystal, the in-plane resistivity ($\rho_{\perp c}$) was measured by a standard four-probe dc technique, but the c -axis resistivity ($\rho_{\parallel c}$) was estimated from measurements using a modified four-probe configuration, with dotlike voltage contacts and with U-shaped current contacts on opposite surfaces.⁹ This method was previously used for layered compounds such as RSb_2 .⁴ However, because of the large anisotropy, it was difficult to determine the absolute value of $\rho_{\parallel c}$. Magnetoresistance measurements were performed in magnetic fields up to 10 T. Magnetization was measured by means of a superconducting quantum interference device magnetometer in fields up to 5.5 T in the temperature range 2–300 K. Specific-heat measurements were carried out by an ac method in fields up to 1 T at temperatures between 0.3 and 20 K. The absolute value of the specific heat was determined by using the value measured by an adiabatic dc method.⁹

III. EXPERIMENTAL RESULTS

The top panel of Fig. 1 shows the isothermal magnetization curves $M(B)$ for a single crystal of CeTe_2 measured in a

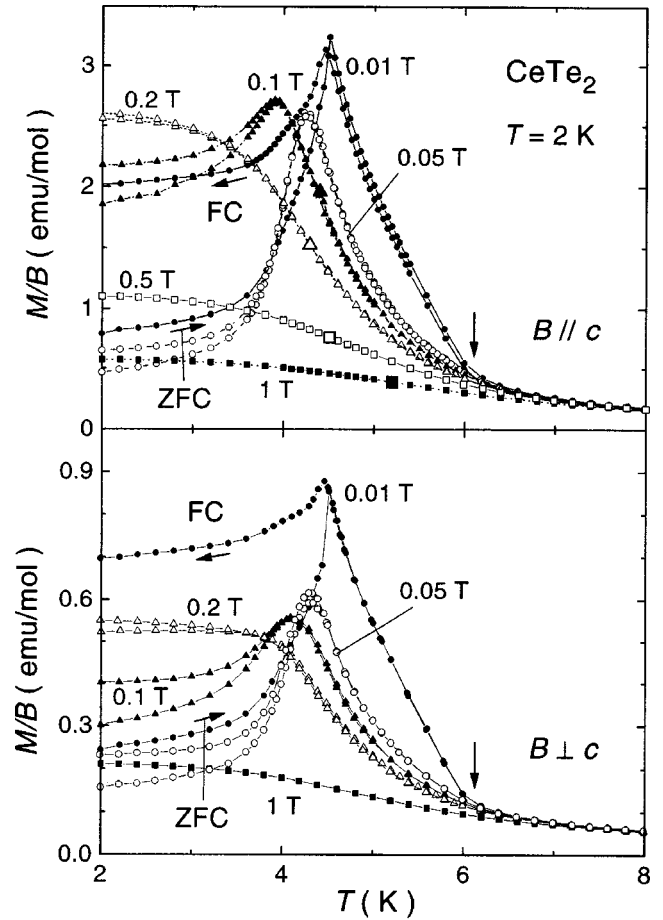


FIG. 2. Temperature dependence of magnetic susceptibility M/B in various magnetic fields for $B\parallel c$ and $B\perp c$ at 2 K for a single crystal of CeTe_2 . The zero-field-cooled (ZFC) and field-cooled (FC) data are compared.

field range $-0.4\leq B\leq 0.4\text{ T}$ for $B\parallel c$ and $B\perp c$. At 2 K, an applied magnetic field of $B_T=0.06\text{ T}$ along the c axis, the easy magnetization direction, induces a metamagnetic transition from the antiferromagnetic state to a field-induced ferromagnetic state. $M(B\parallel c)$ saturates rapidly to a value of $1.0\mu_B/\text{Ce}$ at 0.2 T, whereas $M(B\perp c)$ gradually reaches to a value of $0.3\mu_B/\text{Ce}$ at 0.4 T. It should be noted that a weak hysteresis is observed for both $M(B\parallel c)$ and $M(B\perp c)$ at 2 K. The hysteresis is reduced with increasing temperature, and at 6.1 K $M(B)$ increases linearly without showing hysteresis and remanence.

The temperature dependence of M/B in different magnetic fields for $B\parallel c$ and $B\perp c$ is shown in Fig. 2. In the lowest field of 0.01 T, both M/B curves show a sudden rise at 6.1 K, indicating an onset of ferromagnetic short-range order. It is noteworthy that this temperature coincides with T_p where $\rho(T)$ exhibits a sharp peak. The peak of M/B at $T_N=4.4\text{ K}$ is attributed to the antiferromagnetic long-range order. Only below T_N , there is a significant difference between the zero-field-cooled (ZFC) and field-cooled (FC) data. As the magnetic field is increased up to 0.1 T, the hysteresis is decreased and the peak in M/B shifts to lower temperatures, as expected for an antiferromagnetic transition. Above 0.2 T, the M/B curve steadily increases with decreasing temperature. This behavior is consistent with the field-

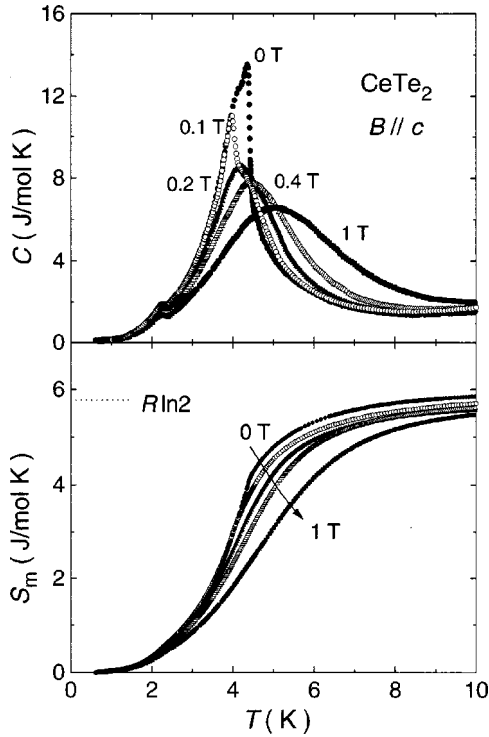


FIG. 3. Temperature dependence of specific heat C (upper panel) and magnetic entropy S_m (lower panel) in various magnetic fields applied along the c axis for a single crystal of CeTe_2 .

induced ferromagnetic state for $B_{\parallel c} \geq 0.2$ T. In the M/B curves, there appears an inflection point, of which the temperature shifts from 4.3 to 5.2 K as the magnetic field increases from 0.2 T to 1 T.

The specific heat $C(T)$ was measured at various magnetic fields applied parallel to the c axis. As is seen in the upper panel of Fig. 3, $C(T)$ in zero field exhibits a pronounced peak centered at 4.3 K. The midpoint of the jump agrees with $T_N = 4.4$ K defined as the peak in the M/B vs T curve. In a field of 0.1 T, the peak shifts down to 4.0 K and furthermore a shoulder appears at 4.3 K. The peak at 4.0 K coincides with the peak temperature observed in M/B at the same field of $B = 0.1$ T, and the shoulder at 4.3 K agrees with the inflection point in the M/B curve. As the field exceeds 0.2 T, the former in $C(T)$ disappears and the latter develops to a broad maximum. With increasing magnetic field further, the maximum temperature T_C shifts to higher temperatures, being characteristic of a ferromagnetic state. The magnetic entropy $S_m(T)$ was estimated by subtracting the $C(T)$ data for LaTe_2 from those for CeTe_2 . The results are displayed in the lower panel of Fig. 3. In zero field, S_m amounts to a value of $0.7R \ln 2$ at $T_N = 4.4$ K and reaches the full value of $R \ln 2$ only at 10 K. The value of S_m decreases gradually with magnetic field and the saturation is achieved well above 10 K. This field variation of $S_m(T)$ is consistent with the stabilization of the ferromagnetic state by applied fields.

Figure 4 shows the temperature dependence of electrical resistivity $\rho(T)$ for $I_{\parallel c}$ and $I_{\perp c}$ measured at constant magnetic fields for $B_{\parallel c}$ and $B_{\perp c}$. The c -axis resistivity $\rho_{\parallel c}$ is much larger than the c -plane resistivity $\rho_{\perp c}$, as was found in the previous measurements using other samples.⁹ However, the ratio $\rho_{\parallel c}/\rho_{\perp c}$ is 45 at 1.5 K, being smaller than that of

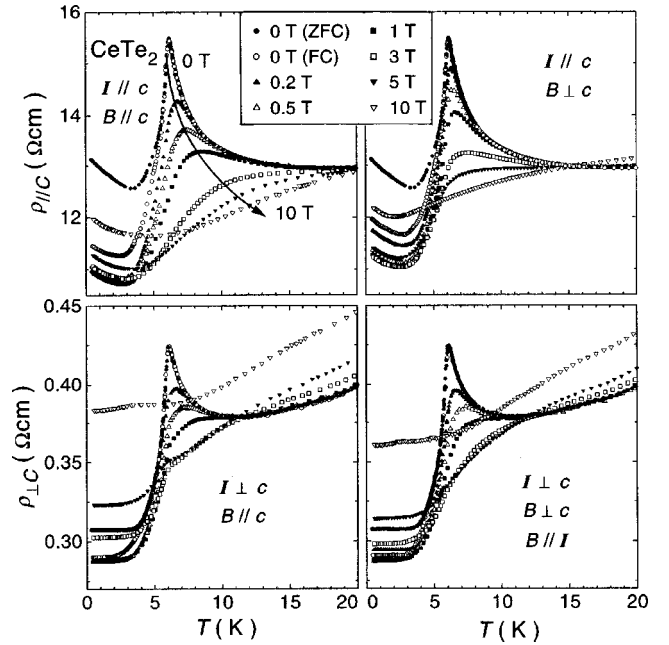


FIG. 4. Magnetic-field variations of electrical resistivity ρ for $I_{\parallel c}$ (upper panels) and $I_{\perp c}$ (lower panels) in fields up to 10 T for $B_{\parallel c}$ (left panels) and $B_{\perp c}$ (right panels) for a single crystal of CeTe_2 .

previous samples. With decreasing temperature below 10 K, both $\rho_{\parallel c}$ and $\rho_{\perp c}$ increase strongly and exhibit a sharp peak at $T_{\rho} = 6.1$ K. The decrease in $\rho(T)$ below T_{ρ} is attributed to the development of ferromagnetic order inferred from the sudden rise of M/B . On further cooling below 3 K, $\rho_{\parallel c}$ increases but $\rho_{\perp c}$ remains constant, as reported previously.⁹ This suggests that the c -axis conduction is suppressed by the antiferromagnetic alignment of CeTe ferromagnetic layers, while the c -plane conduction is not affected. With increasing magnetic field, the peak at T_{ρ} for both $\rho_{\parallel c}$ and $\rho_{\perp c}$ is strongly suppressed and shifts to higher temperatures. This leads to a large negative magnetoresistance in the vicinity of 6.1 K.

Since the field effect on $\rho(T)$ is much different for $I_{\parallel c}$ and $I_{\perp c}$, as shown in Fig. 4, we further measured the field dependence of resistivity $\rho(B)$ up to 10 T at fixed temperatures. In Fig. 5, the results are compared with the $M(B)$ curves. As shown in the top panel, $M(B_{\parallel c})$ at 2 K saturates rapidly to a value of $1.05\mu_B/\text{Ce}$ at $B = 0.2$ T, whereas $M(B_{\perp c})$ increases gradually to a value of $0.75\mu_B/\text{Ce}$ at 5.5 T. As the temperature is raised to 5 K, the saturated moment decreases. In the middle and bottom panels, $\rho(B)$ at 1.5 K initially decreases with fields up to 0.4 T, and then turns to increase making a broad minimum. The magnetoresistance, $\text{MR} = [\rho(B) - \rho(0)]/\rho(0)$, at $B = 0.4$ T is much larger for $I_{\parallel c}$ than for $I_{\perp c}$. This fact suggests that the weak magnetic field affects significantly on c -axis transport, rather than the c -plane one. On the other hand, the positive MR in high magnetic fields is much stronger for $I_{\perp c}$ than for $I_{\parallel c}$. The origin of the positive MR is not clear at present.

In order to find the close relation between $\rho(B)$ and $M(B)$, low-field data of $\rho(B)$ were recorded upon increasing and decreasing magnetic fields. As shown in the middle and bottom panels of Fig. 1, there is marked difference between the ZFC and FC curves at 1.5 K. Even in the FC curves, the

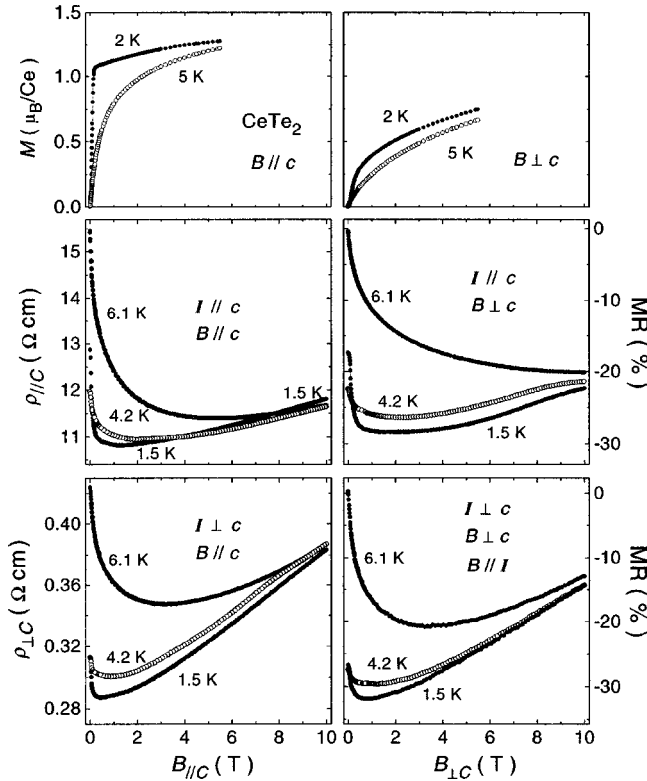


FIG. 5. (Top) isothermal magnetization of a single crystal of CeTe_2 in a field range up to 5.5 T for $B\parallel c$ and $B\perp c$. Magnetoresistance for $I\parallel c$ (middle) and $I\perp c$ (bottom) at 1.5, 4.2, and 6.1 K.

field-up and field-down branches across at $B=0$ and exhibit well-defined symmetric peaks at $B=\pm 0.06$ T. Because this field value coincides with the metamagnetic transition field B_T determined from the $M(B\parallel c)$ curve, the changes in $\rho(B)$ should be associated with the moment orientations in the CeTe double layers. As shown in the top of Fig. 1, the Ce moments are antiparallel in low fields less than ± 0.06 T, while they orient to the field direction as the field exceeds ± 0.2 T. The peak at $B=\pm 0.06$ T in $\rho(B)$ is sharper for $B\parallel c$ than those for $B\perp c$, as similar to the case of the derivative dM/dB at the metamagnetic transition. As the temperature is increased to 4.2 K, the hysteresis in $\rho(B)$ is reduced, and disappears at 6.1 K. In the configuration $I\parallel c$, the negative MR for $B\parallel c$ are twice those for $B\perp c$, while in the configuration $I\perp c$ the MR for $B\parallel c$ and $B\perp c$ are nearly the same. Implications of these observations will be discussed in the next section.

IV. DISCUSSION

We have shown the sets of results of $\rho(T)$, M/B , and $C(T)$ for a single crystal of $\text{CeTe}_{1.85}$ at various magnetic fields. They provide us three characteristic temperatures, T_ρ , T_N , and T_C . We took T_ρ as the peak point in $\rho(T)$. The three-dimensional antiferromagnetic ordering temperature T_N was obtained from the peak point in M/B , which is suppressed in a magnetic field. Above 0.2 T, $M(B\parallel c)$ reaches almost full moment of $1\mu_B/\text{Ce}$, that is expected for a ground state of $J_z = \pm \frac{3}{2}$ for a trivalent Ce ion in the tetragonal crystal field.¹² It should be noted that the inflection point in the M/B vs T curve for $B\parallel c \geq 0.1$ T coincides with T_C , the peak

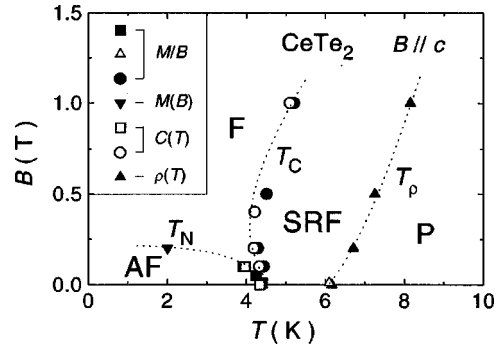


FIG. 6. Magnetic phase diagram (B - T diagram for $B\parallel c$) constructed from the combination of the M/B , $M(B)$, $C(T)$, and $\rho(T)$ data of CeTe_2 . Three transition temperatures, T_ρ , T_N , and T_C , are taken as the peak points in $\rho(T)$, M/B , and $C(T)$ and the inflection points in M/B and $M(B)$, see text. The paramagnetic, short-range ferromagnetic, ferromagnetic, and antiferromagnetic phases are denoted as P, SRF, F, and AF, respectively.

temperature in $C(T)$. Therefore T_C is the transition temperature to the ferromagnetic state which is stabilized by the magnetic field applied along the c axis. Three transition temperatures, T_ρ , T_C , and T_N , are plotted in Fig. 6. The dotted lines are drawn as a guide to the eye. In zero field, the short-range ferromagnetic order develops below T_ρ , which is followed by the antiferromagnetic long-range order below T_N . By applying a magnetic field along the c axis, the transition temperatures are changed: T_N shifts towards lower temperatures, T_C is enhanced, and T_ρ shifts to higher temperatures.

The results described above are consistent with the analysis of elastic and inelastic neutron experiments.^{10,11} The antiferromagnetic structure below $T_N=4.4$ K was determined as follows. The magnetic moments of Ce ions are pointing to the c axis in a CeTe layer, and the ferromagnetic layers are stacked antiferromagnetically in the sequence up-down-Te-down-up along the c axis. In this structure, the semimetallic Te layer is sandwiched by the ferromagnetically coupled CeTe layers, and the semiconducting CeTe double layers are coupled antiferromagnetically. The neutron-scattering experiments have also indicated the presence of another transition at 6.1 K, which agrees with T_ρ determined as the peak in $\rho(T)$. The sudden rise in M/B simultaneously occurring below T_ρ marks the development of two-dimensional ferromagnetic order within the CeTe layer. When such two-dimensional ferromagnetic order develops, the carriers in the semimetallic Te sheet would mediate the ferromagnetic interaction between the two CeTe layers above and below the Te sheet. However, the interlayer exchange interaction within the semiconducting CeTe double layer is antiferromagnetic. This competition between the ferromagnetic and antiferromagnetic exchange interactions may give rise to the actual three-dimensional antiferromagnetic structure built up of the ferromagnetic CeTe layers in the sequence $\uparrow\downarrow\text{Te}\uparrow\downarrow$ along the c axis. This structure changes to the ferromagnetic state by the application of magnetic field above 0.06 T along the c axis, which is reflected in the rapid saturation in the $M(B\parallel c)$ curve.

The metamagnetic transition accompanies a large negative MR, that is displayed in Fig. 1. At 2 K, $M(B\parallel c)$ rapidly increases to a saturated value of $1.0\mu_B/\text{Ce}$ at 0.2 T, whereas

$M(B \perp c)$ increases gradually to a value of $0.3\mu_B/\text{Ce}$ at 0.4 T. Corresponding to this field dependence of $M(B)$, the MR for $B \parallel c$ at 1.5 K in the configuration $I \parallel c$ sharply decreases by about 4.1% with fields up to 0.4 T, whereas the MR for $B \perp c$ decreases by 2.6%. At 6.1 K, the MR further decreases to 14.1 and 7.1% for $B \parallel c$ and $B \perp c$, respectively. This means that the negative MR for $B \parallel c$ is twice that for $B \perp c$ at temperature both below and above T_N . The large negative MR in accordance with the development of $M(B)$ suggests that the electrical conduction is closely related to the spin alignment of Ce ions. When the applied magnetic field overwhelms the antiferromagnetic interlayer coupling, the Ce spins align ferromagnetically along the c axis and thus reduces scattering of the carriers by the Ce spins. However, one should note that the negative MR in CeTe₂ does not obey the scaling function, $\text{MR} \propto -M^2$, which is expected for the conventional MR due to reduced scattering by field alignment of local spins.^{16,17}

Let us now discuss the enhanced MR at $T \sim T_\rho$ observed for the single crystal in the four configurations of B and I . The sharp increase of both $\rho(T)$ and $C(T)$ below 10 K in zero field suggested that the carriers become localized and polarize the neighboring Ce spins ferromagnetically.^{9,12} The formation of a sort of magnetic polarons was also suggested by the observation of a sudden decrease in the unit-cell volume below T_ρ .¹¹ We can thus ascribe the drop in $\rho(T)$ at $T \leq T_\rho$ to the delocalization of carriers by the overlap of the magnetic polarons. A similar mechanism has been proposed to explain the colossal magnetoresistance in manganese perovskites.¹⁸ When a magnetic field above 0.06 T is applied along the c axis, ferromagnetic clusters are oriented in this direction. This enhances the hopping of carriers along the field direction. On the other hand, the c -plane transport may be dominated by the two-dimensional motion of carriers, as is expected from the large anisotropy, $\rho_{\parallel} \gg \rho_{\perp}$. Since the Te sheet is sandwiched by the ferromagnetically coupled CeTe layers in both the antiferromagnetic state and the field-induced ferromagnetic state, the MR for $I \perp c$ could be independent of the field directions.

V. CONCLUSION

For a single crystal of CeTe₂, we have studied the effects of magnetic field on the magnetic susceptibility M/B , specific heat C , and electrical resistivity ρ at various magnetic fields for $B \parallel c$ and $B \perp c$. The combined results allowed us to draw a B - T phase diagram with three characteristic temperatures, T_ρ , T_N , and T_C . With decreasing temperature in zero field, the paramagnetic phase changes to a short-range ferromagnetic state at $T_\rho = 6.1$ K, and then to a three-dimensional antiferromagnetic state below $T_N = 4.4$ K. The application of magnetic field along the c axis, the easy magnetization direction, stabilizes the ferromagnetic phase below T_C , which seems to agree with T_N in zero field. With increasing magnetic field, T_N shifts to lower temperatures, T_C is enhanced, and T_ρ shifts towards higher temperatures. The coincidence of T_C with T_N in zero field indicates that the ferromagnetic interaction between the CeTe layers above and below the Te sheet competes with the antiferromagnetic interaction within the CeTe double layer.

We have observed highly anisotropic behavior in the magnetoresistance. The negative MR is most enhanced near 6.1 K, $\text{MR} \approx -25\%$ at $B_{\parallel c} = 3$ T. In the configuration $I \parallel c$, the changes of MR with fields for $B \parallel c$ and $B \perp c$ correspond to those of $M(B \parallel c)$ and $M(B \perp c)$, respectively, and the MR for $B \parallel c$ is twice that for $B \perp c$. The large MR for $I \parallel B \parallel c$ is a result of the strong reduction of scattering by the ferromagnetic alignment of Ce magnetic moments. In the configuration $I \perp c$, on the other hand, the negative MR for $B \parallel c$ is essentially the same as that for $B \perp c$. This fact supports that the c -plane conduction is dominated by the two-dimensional motion of the carriers within the Te sheet sandwiched by the ferromagnetically ordered CeTe layers.

ACKNOWLEDGMENTS

We are grateful to Professors J. G. Park, Y. S. Kwon, H. Takagi, H. Sato, and T. Kasuya for helpful discussions. The authors thank N. Kikugawa and T. Chihara for their help in the magnetization measurements. The magnetoresistance measurements were performed at the Cryogenic Center, Hiroshima University.

¹E. DiMasi, B. Foran, M. C. Aronson, and S. Lee, Chem. Mater. **6**, 1867 (1994).

²E. DiMasi, M. C. Aronson, B. Foran, and S. Lee, Physica B **206&207**, 386 (1995).

³P. C. Canfield, J. D. Thompson, and Z. Fisk, J. Appl. Phys. **70**, 5992 (1991).

⁴S. S. Bud'ko, P. C. Canfield, C. H. Mielke, and A. H. Lacerda, Phys. Rev. B **57**, 13 624 (1998).

⁵R. Wang, H. Steinfink, and W. F. Bradley, Inorg. Chem. **5**, 142 (1966).

⁶Y. S. Kwon, T. S. Park, K. R. Lee, J. M. Kim, Y. Haga, and T. Suzuki, J. Magn. Magn. Mater. **140-144**, 1173 (1995).

⁷M. H. Jung, Y. S. Kwon, T. Kinoshita, and S. Kimura, Physica B **230-232**, 151 (1997).

⁸M. H. Jung, Y. S. Kwon, and T. Suzuki, Physica B **240**, 83 (1997).

⁹M. H. Jung, B. H. Min, Y. S. Kwon, I. Oguro, F. Iga, T. Fujita, T. Ekino, T. Kasuya, and T. Takabatake, J. Phys. Soc. Jpn. **69**, 937 (2000).

¹⁰J. G. Park, I. P. Swainson, W. J. L. Buyers, M. H. Jung, and Y. S. Kwon, Physica B **241-243**, 684 (1998).

¹¹J. G. Park, Y. S. Kwon, W. Kockelmann, M. J. Bull, I. P. Swainson, K. A. McEwen, and W. J. L. Buyers, Physica B **281-282**, 451 (2000).

¹²T. Kasuya, M. H. Jung, and T. Takabatake (unpublished).

¹³E. DiMasi, B. Foran, M. C. Aronson, and S. Lee, Phys. Rev. B **54**, 13 587 (1996).

¹⁴A. Kikuchi, J. Phys. Soc. Jpn. **67**, 1308 (1999).

¹⁵M. N. Baibich, J. M. Broto, A. Fert, F. Nguyen Van Dau, F. Petroff, P. Eitenne, G. Creuzet, A. Friederich, and J. Chazelas, Phys. Rev. Lett. **61**, 2472 (1988).

¹⁶K. Kubo and N. Ohata, J. Phys. Soc. Jpn. **33**, 21 (1972).

¹⁷A. Urushibara, Y. Moritomo, T. Arima, A. Asamitsu, G. Kido, and Y. Tokura, Phys. Rev. B **51**, 14 103 (1995).

¹⁸J. M. De Teresa, M. R. Ibarra, P. A. Algarabel, C. Ritter, C. Marquina, J. Blasco, J. Garcia, A. del Moral, and Z. Arnold, Nature (London) **386**, 256 (1997).